Improving the Detectability of Highly Coherent Targets in Short-Lag Spatial Coherence Images with Multi-Line Transmission

Giulia Matrone
Dept. of Electrical, Computer and Biomedical Engineering
University of Pavia
Pavia, Italy
giulia.matrone@unipv.it

Muyinatu A. Lediju Bell
Dept. of Electrical and Computer Engineering
Johns Hopkins University
Baltimore, MD, USA
mledijubell@jhu.edu

Alessandro Ramalli
Dept. of Information Engineering
University of Florence
Florence, Italy
alessandro.ramalli@unifi.it

***Abstract*—We hypothesize that the combination of ultrasound Short-Lag Spatial Coherence (SLSC) imaging and Multi-Line Transmission (MLT) can provide enhanced visibility of highly-coherent targets within soft tissues, improving the frame-rate at the same time. Images of a biopsy needle inserted within a lab-made agar/gelatin phantom and an *ex vivo* bovine meat sample were acquired after implementing single-line transmission (SLT) and MLT with an increasing number of simultaneously transmitted beams. The received signals were then beamformed with standard Delay and Sum (DAS) and SLSC algorithms. Results show that MLT SLSC images have darker background than SLT SLSC and DAS B-mode images, which is due to the rapid signal decorrelation at short lags caused by inter-beam interferences. This effect in turn provides increased needle contrast with MLT SLSC imaging, particularly as the number of multiple beams increase, which is promising for a more accurate biopsy needle detection.**

Keywords—Short-Lag Spatial Coherence, Multi-Line Transmission, ultrasound beamforming, biopsy needle, high contrast, high frame-rate.

I. Introduction

Short-Lag Spatial Coherence (SLSC) imaging [1] provides information about the spatial coherence of ultrasound backscattered echoes received by closely spaced elements. Several studies demonstrated its ability to improve image contrast and to suppress clutter, especially in difficult-to-image patients [2].

In this work, we investigate the integration of SLSC with Multi-Line Transmission (MLT) [3], a technique for high frame-rate imaging where multiple beams are transmitted simultaneously. In particular, we hypothesize that this combination can be exploited to enhance the detectability of highly coherent structures within a tissue background. This hypothesis relies on previous analyses published in [4], in which we showed that the pulse-echo beam shape altered by the simultaneous transmission (TX) of multiple beams causes a loss of correlation among echo signals received by the transducer array elements. Spatial coherence drops in the short-lag region, especially as the number of simultaneous TX beams increases.

Thus, our idea is that such a "drawback" could be exploited in SLSC images, which provide a direct mapping of spatial coherence in the image space, yielding in turn an enhanced visibility of highly-coherent targets embedded in soft tissues.

In this paper we show the results of two experiments using a lab-made phantom and a sample of bovine meat to test our hypothesis. In both cases, we inserted into the phantom/meat a needle for percutaneous biopsy and analyzed its contrast when implementing MLT with an increasing number of TX beams, comparing the performance of standard B-mode imaging with Delay and Sum (DAS) beamforming and of SLSC imaging.

II. Methods and Materials

A. Short-Lag Spatial Coherence Imaging

The SLSC algorithm computes the spatial coherence of backscattered ultrasound signals by normalizing their spatial covariance function as follows [1]:

$$R_{SLSC} = \sum_{m=1}^{M} \left[\frac{1}{N-m} \sum_{i=1}^{N-m} \frac{\sum_{n=n_1}^{n_2} s_i(n) s_{i+m}(n)}{\sqrt{\sum_{n=n_1}^{n_2} s_i^2(n) \sum_{n=n_1}^{n_2} s_{i+m}^2(n)}} \right]. \quad (1)$$

In (1), the delayed radiofrequency (RF) signal received by the i-th element in the array is denoted as $s_i(n)$; n represents the time instant index, while $[n_1\ n_2]$ is a small kernel (usually set equal to one wavelength) for coherence averaging. M represents the maximum lag up to which a coherence function is integrated, which can also be expressed as a percentage of the N-element aperture (i.e., $Q=M/N\times100$).

B. Multi-Line Transmission

In MLT imaging, N_B ultrasound beams are transmitted simultaneously, achieving a N_B-factor improvement of the frame-rate [5]. To do so, the transducers are excited with a signal that is obtained by summing up the signals that would be used to focus the beam in each one of the considered TX directions. Inter-beam interferences between the sidelobes and

978-1-7281-5448-0/20/$31.00 ©2020 IEEE

Authorized licensed use limited to: Johns Hopkins University. Downloaded on January 14,2021 at 16:12:29 UTC from IEEE Xplore. Restrictions apply.

the mainlobe of the TX and receive (RX) beams cause artifacts around the point spread function (PSF) main peak [6], whose effect worsens with N_B.

In [4] we demonstrated that the spatial coherence function of signals backscattered by a uniform speckle region around the TX focal depth, which would be almost triangular in the classical single-line transmit (SLT) case [7], is rapidly decreasing in MLT with oscillatory patterns that change with the number of simultaneous transmit beams.

C. Imaging Experiments and Setup

Experiments were performed with the ULA-OP 256 system [8] and a 128-element phased array (model PA230, Esaote s.p.a., Florence, Italy) applying a Hanning-tapered 2-cycle sinusoidal burst, with a 2 MHz center frequency, as the excitation signal. The amplitude of this signal was 64 V. SLT and MLT modes with 4, 8, 16 simultaneous beams (i.e. 4-, 8-, 16-MLT) were implemented on the scanner. Raw channel data were acquired, sampled at 78.125 MHz and transmitted via USB to a computer for offline processing.

Imaging experiments were conducted by scanning a 18G biopsy needle, with 90° insertion angle, first in a non-attenuating 3%-agar 5%-gelatin phantom and then in an *ex vivo* bovine meat sample.

In both cases, ultrasound scans were repeated two times, with and without a metallic wire mesh placed between the phased array and the phantom/meat top surface to generate acoustic clutter [9].

The acquired pre-beamformed RF signals were processed in Matlab (The MathWorks, Natick, MA, USA) to create DAS and SLSC (with Q=50%) images. In SLSC, the [n_1 n_2] kernel length was set to one wavelength.

Needle contrast ratio (CR), defined as in [6], was measured from envelope-detected signals, considering two regions, one within the needle tip and one in the adjacent background.

III. Results and Discussion

In Fig. 1, the transversal views of the biopsy needle inserted in the agar/gelatin phantom are shown, both with DAS and SLSC, without and with the metallic wire mesh. Fig. 2 instead reports images obtained using the meat sample. The CR values measured in these two scenarios are finally plotted in Fig. 3.

By looking at SLSC images in all the considered cases, it can be immediately noticed that, as the number of simultaneously transmitted beams increases, the background darkness increases, and thus the visibility of the needle is improved. A strong comet-tail artifact is also visible in the absence of clutter and the artifact is least obvious in MLT SLSC images with clutter. On the other hand, we can see that generally, in DAS B-mode images with MLT, crosstalk artifacts appear and their presence (i.e., the sidelobes at the left and right sides of the needle) is stronger as the number of TX beams increases. This effect would be even more evident when increasing the dynamic range used for image display.

The effect of clutter generated by the metallic wire mesh is clearly visible in Fig. 1, where the background of DAS images is much more filled up as compared to the without-clutter case. For what concerns SLSC, adding clutter makes this technique work even better: as it can be seen in Fig. 1, the background in SLSC images looks almost completely black when clutter is added, and thus contrast is higher than in the case without the clutter-generating wire mesh.

The measured CR values in Fig. 3 for the agar/gelatin phantom show that contrast increases with N_B for SLSC images, while it has a decreasing trend in DAS images. However, when no clutter is present, DAS consistently

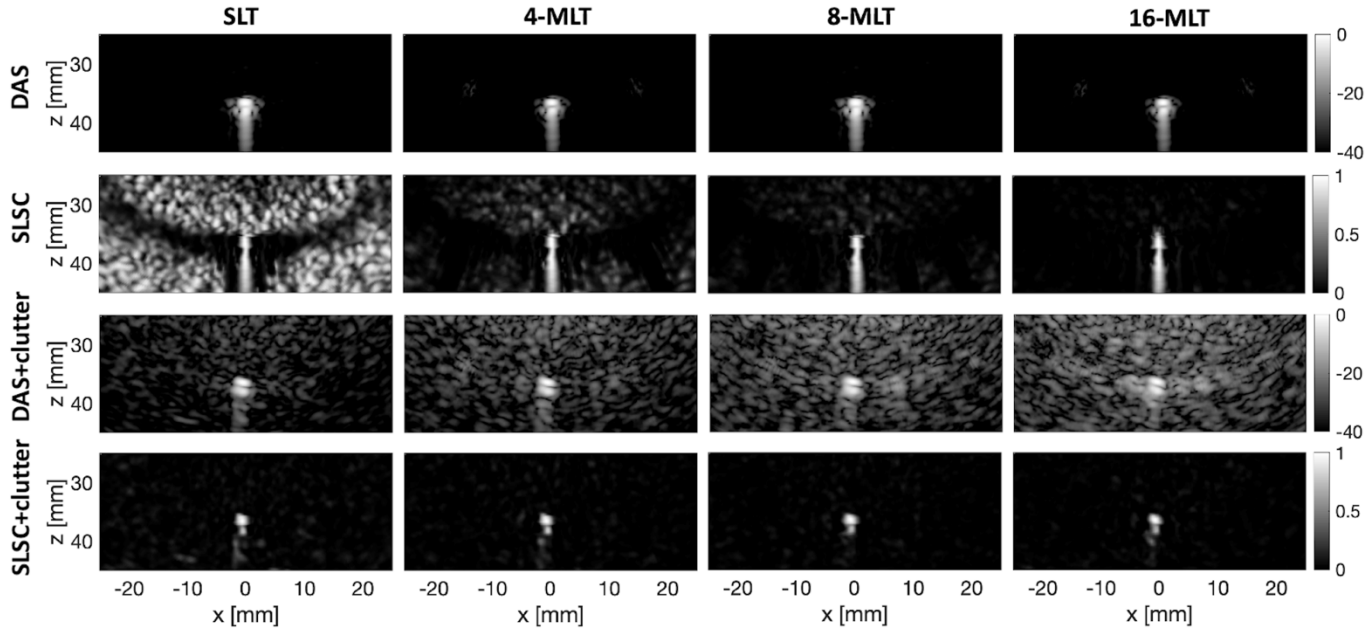

Fig. 1. SLT and MLT images of the biopsy needle inserted transversally into the agar/gelatin phantom, without (top rows) and with (bottom rows) the wire mesh, obtained with DAS and SLSC (Q=50%) imaging. DAS images are displayed over a 40 dB dynamic range, while SLSC images are on a [0,1] linear scale.

Authorized licensed use limited to: Johns Hopkins University. Downloaded on January 14,2021 at 16:12:29 UTC from IEEE Xplore. Restrictions apply.

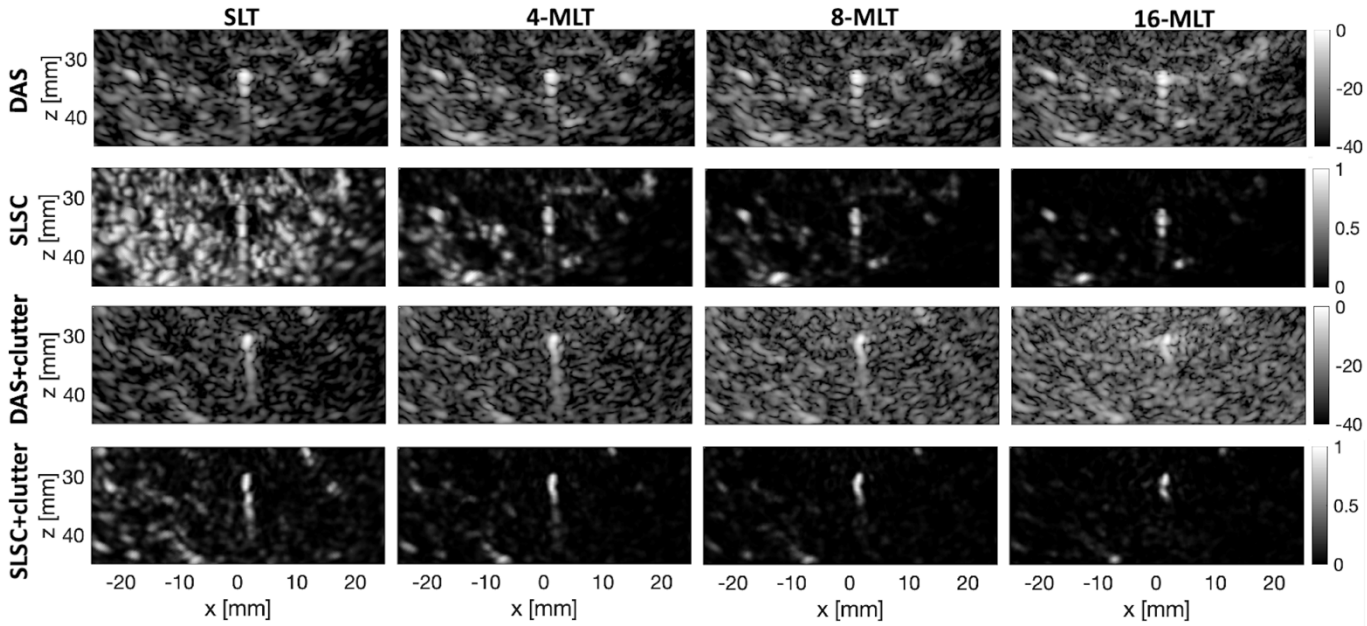

Fig. 2. SLT and MLT images of the biopsy needle inserted transversally into the meat sample, without (top rows) and with (bottom rows) the wire mesh, obtained with DAS and SLSC (Q=50%) imaging. DAS images are displayed over a 40 dB dynamic range, while SLSC images are on a [0,1] linear scale.

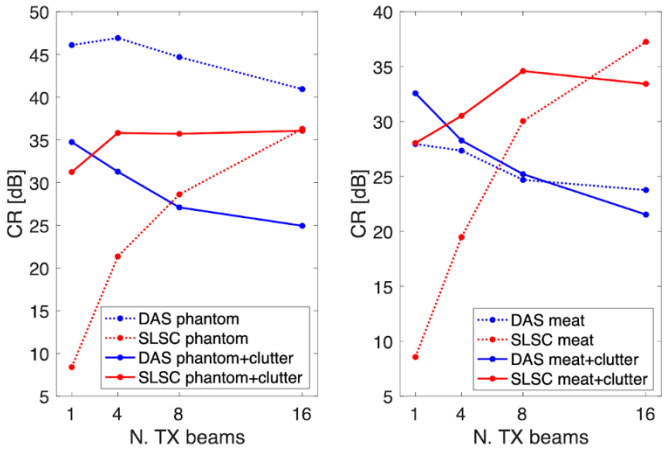

Fig. 3. Measured CR values for the needle in the agar/gelatin phantom (left) and in the bovine meat sample (right).

outperforms SLSC, while with clutter and MLT the performance of SLSC is higher. For example, with clutter present, the CR of the 16-MLT SLSC image is 36 dB, which is ~11 dB higher than that of the 16-MLT DAS image, and similar to that of the SLT DAS image (~15 dB), but with a 16 times higher frame-rate.

Regarding acquisitions with the meat sample, Fig. 2 again shows that with MLT SLSC the background darkness increases, particularly when the wire mesh is applied creating acoustic clutter in the image. On the other hand, DAS images are affected by crosstalk and clutter that degrade the CR as the number of TX beams increases.

For N_B>4, SLSC provides a higher CR than DAS even in the case without added clutter (Fig. 3). When clutter is present, all considered MLT configurations have higher CR when compared to the corresponding DAS CR values. For example, the 16-MLT SLSC image with clutter has ~12 dB and ~1 dB higher CR than that in 16-MLT DAS and SLT DAS images with clutter, respectively. These differences increase to 13.5 dB and ~9 dB, respectively, in the no-clutter case. Note that employing MLT and SLSC can bring not only an enhancement of the needle visibility/contrast, but also an improvement of the frame-rate.

IV. Conclusion

MLT SLSC images show a darker background than SLT SLSC images, particularly when clutter is present, considering the rapid decorrelation that occurs at short lags with MLT. The decorrelation effect due to MLT can be exploited to achieve high-frame-rate, high-contrast images of highly coherent targets, which is beneficial for ultrasound-guided biopsies performed on otherwise difficult-to-image patients.

Acknowledgment

The authors thank Dr. P. Della Vigna (European Institute of Oncology, Milan, Italy) for the fruitful discussion on biopsy-needle ultrasound imaging.

References

[1] M. A. Lediju, G. E. Trahey, B. C. Byram, and J. J. Dahl, "Short-lag spatial coherence of backscattered echoes: imaging characteristics," *IEEE Trans. Ultrason., Ferroelectr., Freq. Control*, vol. 58, no. 7, pp. 1377–1388, 2011, doi: 10.1109/TUFFC.2011.1957.

[2] J. J. Dahl, D. Hyun, M. Lediju, and G. E. Trahey, "Lesion detectability in diagnostic ultrasound with short-lag spatial coherence imaging," *Ultrason Imaging*, vol. 33, no. 2, pp. 119–133, Apr. 2011, doi: 10.1177/016173461103300203.

[3] L. Tong, A. Ramalli, R. Jasaityte, P. Tortoli, and J. D'hooge, "Multi-transmit beam forming for fast cardiac imaging--experimental validation and in vivo application," *IEEE Trans. Med. Imaging*, vol. 33, no. 6, pp. 1205–1219, 2014, doi: 10.1109/TMI.2014.2302312.

[4] G. Matrone and A. Ramalli, "Spatial Coherence of Backscattered Signals in Multi-Line Transmit Ultrasound Imaging and Its Effect on Short-Lag

Authorized licensed use limited to: Johns Hopkins University. Downloaded on January 14,2021 at 16:12:29 UTC from IEEE Xplore. Restrictions apply.

Filtered-Delay Multiply and Sum Beamforming," *Applied Sciences*, vol. 8, no. 4, p. 486, Apr. 2018, doi: 10.3390/app8040486.

[5] L. Tong, H. Gao, and J. D'hooge, "Multi-transmit beam forming for fast cardiac imaging--a simulation study," *IEEE Trans. Ultrason., Ferroelectr., Freq. Control*, vol. 60, no. 8, pp. 1719–1731, Aug. 2013, doi: 10.1109/TUFFC.2013.2753.

[6] G. Matrone, A. Ramalli, A. S. Savoia, P. Tortoli, and G. Magenes, "High Frame-Rate, High Resolution Ultrasound Imaging With Multi-Line Transmission and Filtered-Delay Multiply And Sum Beamforming," *IEEE Trans. Med. Imaging*, vol. 36, no. 2, pp. 478–486, Feb. 2017, doi: 10.1109/TMI.2016.2615069.

[7] R. Mallart and M. Fink, "Adaptive focusing in scattering media through sound-speed inhomogeneities: The van Cittert Zernike approach and focusing criterion," *J. Acoust. Soc. Am.*, vol. 96, no. 6, pp. 3721–3732, 1994, doi: 10.1121/1.410562.

[8] E. Boni *et al.*, "ULA-OP 256: A 256-Channel Open Scanner for Development and Real-Time Implementation of New Ultrasound Methods," *IEEE Transactions on Ultrasonics, Ferroelectrics, and Frequency Control*, vol. 63, no. 10, pp. 1488–1495, Oct. 2016, doi: 10.1109/TUFFC.2016.2566920.

[9] M. A. Lediju Bell and J. Shubert, "Photoacoustic-based visual servoing of a needle tip," *Scientific Reports*, vol. 8, no. 1, p. 15519, Oct. 2018, doi: 10.1038/s41598-018-33931-9.

Authorized licensed use limited to: Johns Hopkins University. Downloaded on January 14,2021 at 16:12:29 UTC from IEEE Xplore. Restrictions apply.